

Robotic Harvesting of Rosa Damascena Using Stereoscopic Machine Vision

¹Armin Kohan, ¹Ali Mohammad Borghae, ²Mehran Yazdi,
³Saeid Minaei and ⁴Mohammad Javad Sheykhdavudi

¹Department of Agricultural Machinery Eng., College of Agriculture,
Science and Research Branch, Islamic Azad University (IAU), Tehran, Iran

²Department of Communications and Electronics Eng.,

School of Electrical and Computer Eng., College of Eng., Shiraz University, Shiraz, Iran

³Department of Agricultural Machinery Eng., College of Agriculture, Tarbiat Modares Univ., Tehran, Iran

⁴Department of Agricultural Machinery Eng., College of Agriculture, Chamran Univ., Ahvaz, Iran

Abstract: In this paper, we propose a system for the automated harvest of Rosa Damascena by aid of computer vision techniques. Three dimensional positions of flowers are obtained by stereo vision technique. For harvesting flowers a four-DOF manipulator is used. Also, an end-effector is designed to harvest the flowers by cutting them. To analyze the stereoscopic error, a factorial experiment in the form of a completely randomized design with 2 factors was conducted. The first factor was the distance between cameras at the three levels of 5,10 and 20cm and the second factor was the distance between the camera and the flower at the four levels of 50,75,100 and 125cm. The analysis was done using Duncan's Multiple Range Test at the 1% level. We concluded that the increase in the distance between the cameras reduces the stereoscopic error, while the increase in the distance between the cameras and the flowers increases the error. Finally, the manipulator and the vision system were evaluated altogether. The best results were obtained when the relative distance between cameras was 100 mm. In this case, 82.22 percent of the flowers were successfully harvested.

Key words: Rosa Damascena harvester • Stereo vision • Robotic harvesting • Image processing

INTRODUCTION

Rosa Damascena, more commonly known as the Damask rose, is a member of the family Rosaceae. It is used in various industries such as pharmaceutical, cosmetics, perfumery and food. Harvesting begins from April to May and flowers are picked from where the stem connects to sepal. Picking is done by human labor under blazing sun and it is extremely intensive labor. Because of tedious and repetitive tasks, already, researches were focused on the automation of agricultural and horticultural crop production many years ago.

[1] Developed a watermelon-harvesting robot. To pick up a fruit, the relative positions of the fruit and the manipulator were detected using the stereo image method. [2] presented an image processing system for conducting an orange picking robot. [3] applied machine vision and

image analysis algorithms for mushroom location and seizing and showed the possibility of using a robot to harvest mushrooms for the fresh market.

[4] developed a system for the automated harvest of *Gerbera jamesonii* pedicels with the help of image analysis techniques. Images of plants were taken with a stereo camera system, which consisted of two CCD-cameras with near-infrared filters. The plant was placed on a rotatable desk and images of eight different locations were taken. Three-dimensional models of the pedicels were created by a triangulation process.

[5] developed an image processing method to detect green citrus fruit in individual trees. A hyperspectral camera of 369-1042 nm was employed to acquire hyperspectral images of green fruits of three different citrus varieties and by the means of these images green citrus fruits were detected.

Van Henten *et al.* [6] developed an autonomous robot for harvesting cucumbers in greenhouses. Two camera vision systems were employed for creating 3D images of the fruit and the environment. A control scheme was used to generate collision free motions for the manipulator during harvesting. The manipulator had seven degrees of freedom. The proposed computer vision system was able to detect more than 95% of the cucumbers in a greenhouse.

Tanigakia *et al.* [7] Manufactured a cherry-harvesting robot for trial purposes. The main parts of the robot were a manipulator with 4 degrees of freedom, an 3-D vision sensor, an end effector, a computer and a moving device. The 3-D vision sensor was equipped with red and infrared laser diodes. Both laser beams scanned objects simultaneously. By processing the images obtained from the 3-D vision sensor, the location of the fruits and obstacles was recognized and the trajectory of the end effector was determined. Fruits were picked by the end effector and collisions with obstacles were efficiently avoided.

Noordam *et al.* [8] Evaluated computer vision methods like stereo imaging, laser triangulation, Rontgen imaging and reverse volumetric intersection, to determine which method is the most practicable for locating the stem and tracking the stem down to locate the cutting position. They concluded that reverse volumetric intersection is the best method to locate the stem cutting position in terms of robustness and costs.

In the present work, a machine vision for harvesting Rosa Damascena flower using stereoscopic technique is designed. The harvester only harvests the flower for industrial usage and the position of the stem is not important.

MATERIALS AND METHODS

Vision System: The vision system includes two CCD-cameras forming a stereovision system that can move along the horizontal axis relatively. A portable computer is used to run the implemented programs for camera calibration, image rectification, object recognition and matching stereo images.

Camera Calibration: It is an important pre-step in correctly matching the stereo images and in precisely computing the depth in the stereovision system. It is the process of estimating intrinsic and extrinsic parameters of the camera to minimize the discrepancy between the observed image features and their theoretical positions in the camera pinhole model. Camera calibration in the present study was done based on [9, 10].

Rectification: For a given point in one image, we have to search for its correspondent in the other image along an epipolar line [11]. Generally, epipolar lines are not aligned with the coordinate axis and are not parallel. Such searches are time consuming since we must compare pixels on skew lines in the image space. These types of algorithm can be simplified and made more efficient if epipolar lines are axis aligned and parallel so that epipolar lines in the original images map to horizontally aligned lines in the transformed images. This can be realized by applying 2D projective transforms to each image. This process is known as image rectification [12]. Calibrating the stereo rig leads to a simpler technique for rectification. Figure 1 shows original stereo images after calibration and rectification. Rectification process was done based on [13].

Object Recognition: Considering the flower's color being different from that of the foliage, the best space for detecting the flowers was HSI (Hue-Saturation-Intensity) color space. Since the H- component has the data on the image color (Figure 2b), by thresholding this component, the flowers can be marked in the image.

After thresholding the image, a binary image is obtained. By using the opening operator [14] on the image once and removing the noise, better distinct regions in the image are obtained (Figure 2c). In this stage, all the existing regions are labeled and several times erosion operator followed by dilation operator [14] are applied. Whenever one region is separated into two new regions, the previous region is replaced by these two regions in the binary image. In this way, the flowers that are partially overlapped are detected and distinguished. Figures 2d, 2e and 2f show an example of this case and how we process it. Finally, the coordinates of the region centers in both stereo images are extracted and used later to determine the 3D position of flowers.

Matching: Once an image has been segmented, the shape of objects and epipolar constrains are used to identify best matches between the stereo images. If there are more than one point on the epipolar line of the two images, then objects located on the same epipolar line from two images are superposed onto each other at the centeroid and the union size is calculated by identifying pixels contained in both images. If there is a minimum percentage of pixel overlap, then the two objects are identified as a stereo pair. Ordering constrain is used too. This constrain indicates that, points in the right image have the same order in the left image. After matching, the 3D coordinates of the flower obtained by stereo triangulation [15].

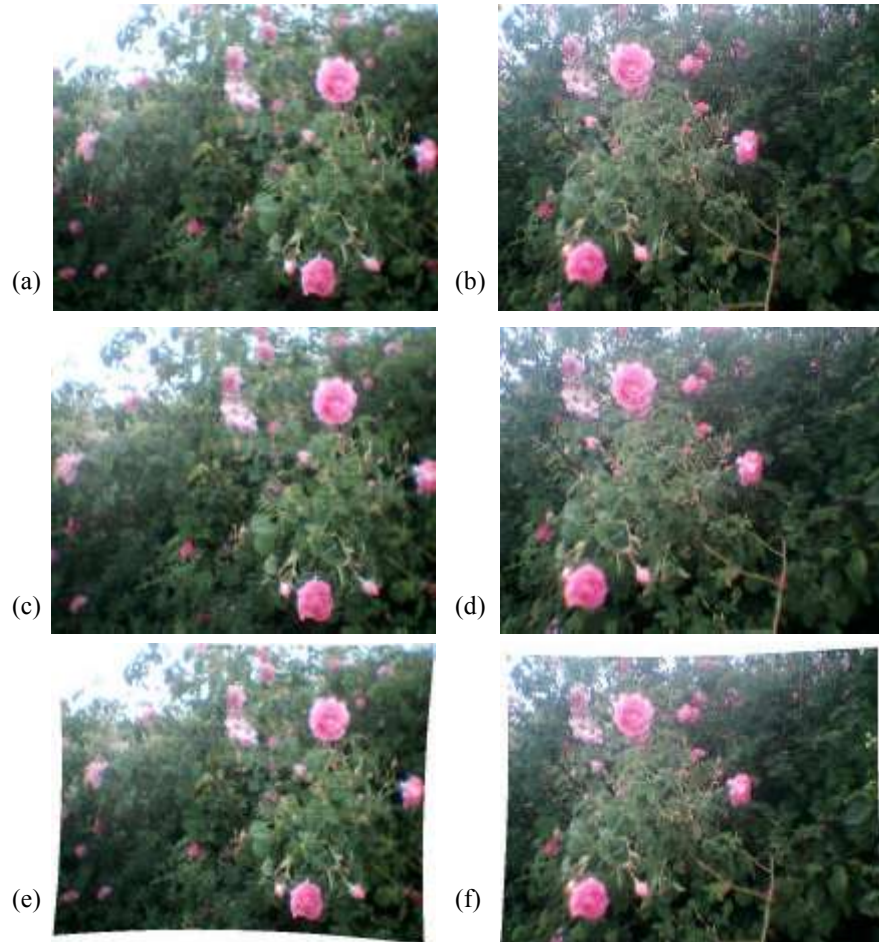


Fig. 1: Calibration and rectification on a tested image; a) and b) are original left and right images, c) and d) are calibrated left and right images, e) and f) are rectified left and right images respectively.

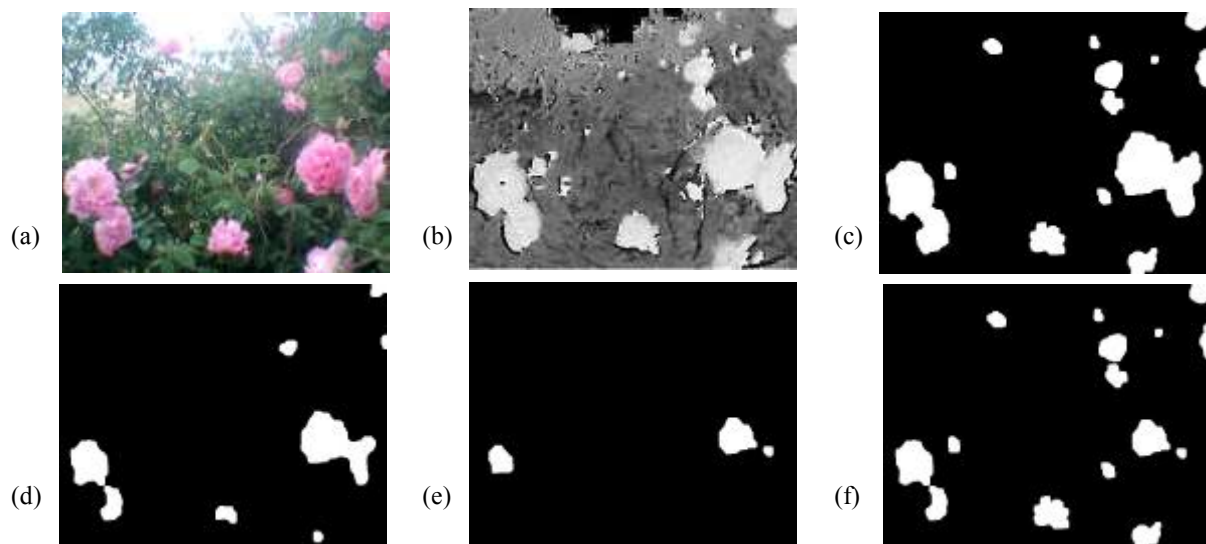


Fig. 2: a) a tested flower image, b) H-component of the HSI image, c) image b after applying the threshold and opening operator once, d) image c after applying several times consecutive erosion and dilation operators, e) image c after applying 8 times consecutive erosion and dilation operators, f) final image after considering all found regions



Fig. 3: The manipulator



Fig. 4: Images taken from end effector

Vision System Evaluation: For a better analysis of the stereoscopic depth measurement error, a factorial experiment in the form of a completely randomized design with 21 replications was conducted. The experiment had two factors. The first factor was the distance between cameras at the three levels of 50,100 and 200mm and the second factor was the distance between the camera and

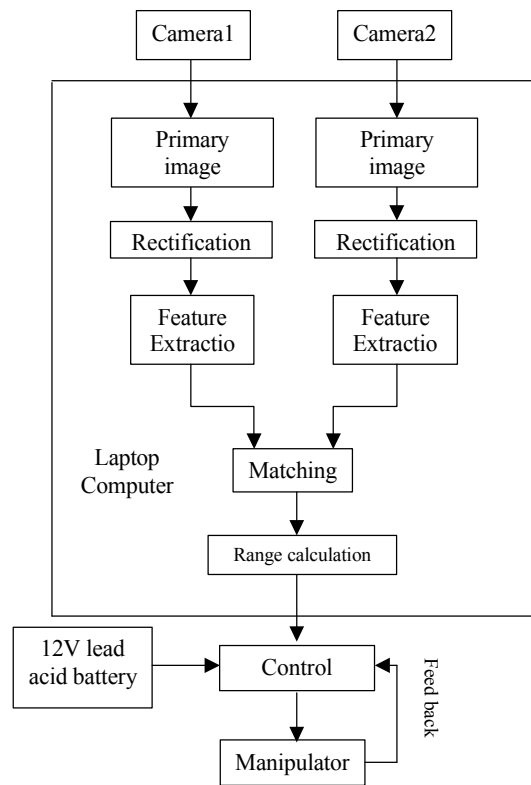


Fig. 5: Block diagram of the harvester

the flower at the four levels of 500, 750, 1000 and 1250mm. The output of experiments, after assessing the variance (Table 1), was analyzed using Duncan's Multiple Range Test at the 1% level.

Robotic Harvesting: A four degree freedom manipulator for picking flowers was designed and mounted (Figure 3). Four DC motors that guide the manipulator to the desired position were equipped with a potentiometer. A special clipper for picking flowers was designed and mounted (Figure 4). The Clipper has a curved form. It has two appendages which are covered with soft rubber to keep the flower after picking. The clipper was designed to be moved by an DC motor. After being picked, flowers are placed at the site of collecting flowers by the manipulator. The control commands required to carry out the harvesting operation were supplied to the manipulator control circuit via the serial port of the computer. Figure 5 shows the block diagram of the harvester.

RESULTS AND DISCUSSION

For the purpose of evaluating the image processing algorithms, 30 stereo images were tested. Incorporating 181 flowers in total in all images, 98% of the flowers present in the images were detected correctly. Certain flowers were not detectable since a major part of them was covered by the foliage.

As Table 1 shows, the analysis of the variance and F-test indicates that the effect of depth variation and cameras relative distance on the depth measurement error by stereoscopy is significant. Analysis by Duncan’s Multiple Range Test (Tables 2, 3 and 4) show that, generally increasing the distance between the cameras reduces the stereoscopic error, while increasing the distance between the stereo cameras and the flowers increases it.

The errors along the axes Y and X are shown in Tables 5 and 6, respectively for different values for the Z. The results show that the error and its variance are increased either we augment the distance between a target object from the cameras or increase the distance between two cameras.

The results on matching process show that an increase in the distance between cameras causes that the risk of having the occlusion between objects increases and the matching becomes more difficult since two images from two camera are less similar. Consequently, the error in matching the images increases. The percent of those errors in different treatments are shown in Table 7. By moving the camera away from the shrub, the number of

Table 1: Analysis of variance of the error of depth measurement by stereoscopy.

	DF	SS	MS	FS
Treatment	11	65452.13	5950.19	374.94*
Depth	3	31222.35	10407.45	655.80*
Cameras relative distance	2	25304.22	12652.11	797.24*
Interaction	6	8925.556	1487.593	93.73*
Error	240	3808.76	15.87	
Total	251	69260.89		

* denotes that the F-test is significant at 1% level

Table 2: Effect of depth variation on the mean of depth measurement error (all means are significantly different at the 1% level according to Duncan’s Multiple Range Test).

Depth(mm)	500	750	1000	1250
Depth measurement mean error(mm)	6.43	13.1	24.4	35.63

Table 3: Effect of the variation in distance between two cameras on the mean of depth measurement error (all means are significantly different at the 1% level according to Duncan’s Multiple Range Test.)

Cameras relative distance (mm)	50	100	200
Depth measurement mean error(mm)	33.5	16.5	9.67

Table 4: Effect of variation in distance between two cameras and that between the camera and the object on the mean of depth measurement error by stereoscopy (the means that are associated with the same letters, do not have a significant difference at the 1% level.)

Cameras relative distance (mm)	50				100				200			
	500	750	1000	1250	500	750	1000	1250	500	750	1000	1250
Depth measurement mean error(mm)	10.14b	22.10c	41	60.76	5.57a	10.48b	20.81c	29.14	3.57a	6.71a	11.38b	17.00

Table 5: Errors in the direction of Y axis

Cameras relative distance (mm)	50				100				200			
depth (mm)	Z=500	Z=750	Z=1000	Z=1250	Z=500	Z=750	Z=1000	Z=1250	Z=500	Z=750	Z=1000	Z=1250
Average of error (mm)	2.38	4.48	9.81	12.67	2.05	3.19	5.9	8.14	0.86	2.1	3.62	5.1
Error variance	1.45	2.36	3.26	5.43	0.95	1.66	4.59	6.23	0.53	1.69	3.85	4.09

Table 6: Errors in the direction of X axis

Cameras relative distance (mm)	50				100				200			
depth (mm)	Z=500	Z=750	Z=1000	Z=1250	Z=500	Z=750	Z=1000	Z=1250	Z=500	Z=750	Z=1000	Z=1250
Average of error (mm)	2.71	4.57	9.57	13.43	2.14	3.29	6.05	9.14	1.62	2.57	4.52	6.81
Variance	1.61	2.26	3.56	4.96	1.43	2.01	3.05	4.23	1.25	1.76	2.86	3.66

Table 7: Errors during matching process

Cameras relative distance (mm)	I=50				I=100				I=200			
Depth (mm)	Z=500	Z=750	Z=1000	Z=1250	Z=500	Z=750	Z=1000	Z=1250	Z=500	Z=750	Z=1000	Z=1250
Percent of unmatched objects	6.25	7.77	9.14	10.03	8.62	11.86	22.75	26.46	15.94	21.49	33.33	39.59

Table 8: Percentage of the success and failure in the harvest

Cameras relative distance (mm)	50		100		200	
Harvesting failure	Number	43	32	46		
	Rate	23.88	17.77	45.55		
Successfully harvested	Number	137	148	134		
	Rate	76.11	82.22	74.44		

flowers in the captured image increased and consequently the matching error increased due to the fact that flowers became more similar.

Finally, the performance of harvester was evaluated by varying the distance between the cameras. In each variation, 180 flowers were considered for harvesting. The obtained results are shown in Table 6. During harvesting, the distance between the stereo rig and shrub was kept 500 to 750 mm. The best results were obtained when the distance between the cameras was 100 mm. According to Tables 2 and 7, although in this case the number of matching errors was increased but positioning error was reduced. According to Table 7, the matching error in this case, was less than the case that the distance between the cameras was 200 mm.

REFERENCES

1. Umeda, M., S. Kubota. and M. Iida. 1999. Development of "STORK", a watermelon-harvesting robot. *Artif. Life Robotics*, 3: 143-147.
2. Plebe, A. and G. Grasso, 2001. Localization of spherical fruits for robotic harvesting. *Machine Vision and Applications*, 13(2): 70-79.
3. Reed, J.N., S.J. Miles, J. Butler, M. Baldwin and R. Noble, 2001. Automatic mushroom harvester development. *J. Agricultural Engineering Res.*, 78 (1): 15-23.
4. Rath, T. and M. Kawollek, 2009. Robotic harvesting of Gerbera Jamesonii based on detection and three-dimensional modeling of cut flower pedicels. *Computers and Electronics in Agric.*, 66: 85-92.
5. Okomoto, H. and W.S. Lee, 2009. Green citrus detection using hyperspectral imaging, *Computers and Electronics in Agric.*, 66: 201-208
6. Van Henten, E.J., J. Hemming, B.A.J. Van Tuijl, J.G. Kornet, J. Meuleman, J. Bontsema and E.A. Van Os, 2002. An autonomous robot for harvesting cucumbers in greenhouse. *Autonomous Robots*, 13(3): 241-258.
7. Tanigakia, K., T. Fujiura, A. Akaseb and J. Imagawa, 2008. Cherry-harvesting robot. *Computers and Electronics in Agric.*, 63: 65-72.
8. Noordam, J.C., J. Hemming, C. Van Heerde, F. Goldbach, R. van Soest and E. Wekking, 2005. Automated rose cutting in greenhouses with 3d vision and robotics: analysis of 3d vision techniques for stemdetection. *Acta. Horticulturae*, 691: 885-892.

9. Heikkila, J. and O. Silven, 1997. A four-step camera calibration procedure with implicit image correction. In the Proceedings of the IEEE Computer Society Conference on Computer Vision and Pattern Recognition, pp: 1106-1112.
10. Zhang, Z.Y.. 1999. Flexible camera calibration by viewing a plane from unknown orientations. In the Proceedings of the IEEE Conference on Computer Vision, 1: 666-673.
11. Zhang. Z., 1998. Determining the epipolar geometry and its uncertainty: A review. *International J. Computer Vision*, 27(2): 161-1195.
12. Loop, C. and Z. Zhang, 1999. Computing rectifying homographies for stereo vision. In the Proceedings of the IEEE Computer Society Conference on Computer Vision and Pattern Recognition, 1: 125-131.
13. Fusiello, A., E. Trucco and A. Verri, 2000. A compact algorithm for rectification of stereo pairs. *Machine Vision and Application*, 12: 16-22.
14. Gonzalez, C., R.E. Woods and S.L. Eddins, 2004. *Digital image processing using matlab*. New Jersey: Pearson Education Inc.,
15. Forsyth, A.F. and J. Ponce, 2006. *Computer Vision A Modern Approach*. Prentice Hall of India.